

PREPARATORY WORK FOR A FLUORESCENCE BASED PROFILE MONITOR FOR AN ELECTRON LENS

S. Udrea[†], P. Forck, GSI Helmholtzzentrum für Schwerionenforschung, Darmstadt, Germany
 E. Barrios Diaz, O. R. Jones, P. Magagnin, G. Schneider, R. Veness, CERN, Geneva, Switzerland
 V. Tzoganis, C. Welsch, H. Zhang, Cockcroft Institute, Warrington, United Kingdom

Abstract

A hollow electron lens system is presently under development as part of the collimation upgrade for the high luminosity upgrade of LHC. Moreover, at GSI an electron lens system also is proposed for space charge compensation in the SIS-18 synchrotron to decrease the tune spread and allow for the high intensities at the future FAIR facility. For effective operation, a very precise alignment is necessary between the ion beam and the low energy electron beam. For the e-lens at CERN a beam diagnostics setup based on an intersecting gas sheet and the observation of beam induced fluorescence (BIF) is under development within a collaboration between CERN, Cockcroft Institute and GSI. In this paper we give an account of recent preparatory work with the aim to find the optimum way of distinguishing between the signals due to the low energy electron beam and the relativistic proton beam.

BIF SETUP FOR TRANSVERSE DIAGNOSTICS

Electron lenses (e-lens) [1] have been proposed and used to mitigate several issues related to beam dynamics in high current synchrotrons. The e-lens system at CERN will be comparable to those used at FNAL and BNL. The main difference will be the use of a hollow electron beam.

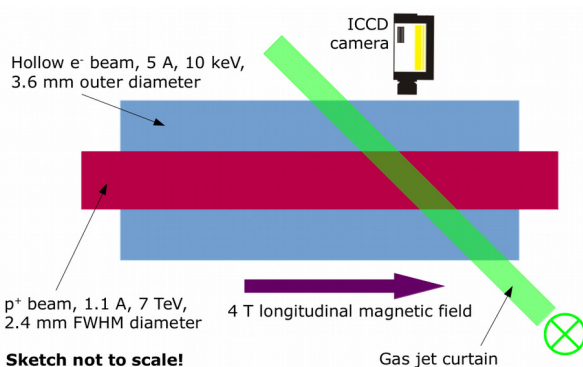


Figure 1: A schematic of the e-lens system planned at CERN for the collimation of the HL-LHC proton beam and the associated transverse beam diagnostics.

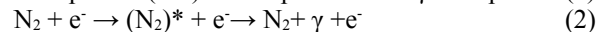
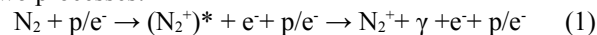
The parameters of the CERN e-lens are summarized in Fig. 1: the up to 1.1 A, 7 TeV, 2.4 mm FWHM diameter proton beam of the HL-LHC will be embedded in an up to 5 A, 10 keV hollow electron beam with an outer diameter of about 3.6 mm and an inner one of 2.4 mm. The interaction between the two beams takes place within an approximately 4 T longitudinal magnetic field, which

stabilizes the electron beam. The proposed beam induced fluorescence (BIF) setup is composed of a perpendicular supersonic gas jet curtain [2] inclined such as to allow for the observation of the fluorescence radiation resulting from the interaction of the electron and proton beams with the gas molecules. To obtain an image of the transverse profiles of the beams a camera system with suitable optics is intended, which consists of an image intensifier made of micro channel plates (MCP) in chevron configuration and a CCD camera with appropriate optics.

RELEVANT FLUORESCENCE PROCESSES

From detection perspective the most appropriate gas to be employed in the supersonic gas jet curtain is nitrogen [3]. The main reasons are its high fluorescence efficiency and, based on present knowledge, it may allow distinguishing between the electron and the proton beam.

At wavelengths in the range 300–700 nm most of the fluorescence of N_2 molecules and N_2^+ molecular ions excited and ionized by protons or electrons results from two processes:



The first one is based on the electronic transition $B^2\Sigma_u^+ \rightarrow X^2\Sigma_g^+$ of the molecular ion with wavelengths around 391 nm (depending upon involved vibrational and rotational states) while the second process drives the electronic transition $C^3\Pi_u \rightarrow B^3\Pi_g$ of the neutral molecule with wavelengths around 337 nm. Moreover, the second process cannot be initiated directly by protons because it implies a spin flip mechanism. Thus one expects different photon intensities in the two spectral regions within the area excited by the proton and ion beams, respectively.

CROSS-SECTIONS AND INTEGRATION TIMES

Proton Excitation

Data for fluorescence from N_2 at relativistic proton energies is provided in [4]. There it is shown that the change of the emission cross-sections with energy closely follows the proton's energy loss as described by a Bethe-Bloch-like expression. From this data one can extrapolate the cross-section at 7 TeV proton energy by the following expression:

$$\sigma_p = A_1 \cdot [(1 + e^{-x}) \cdot (x + B_1) - 1] \quad (3)$$

with $A_1 = 1.789 \cdot 10^{-21} \text{ cm}^2$, $B_1 = 10.3$, $x = 2 \cdot \ln(p \cdot c / E_0)$, $E_0 = 0.938 \text{ GeV}$ – rest energy of the proton – and $p \cdot c$ the proton's momentum. At LHC maximum energy $p \cdot c \approx 7 \text{ TeV}$ resulting in $\sigma_p \approx 3.4 \cdot 10^{-20} \text{ cm}^2$, with a 70 % correction made for the main transition of the N_2 ion.

[†]email address s.udrea@gsi.de

Electron Excitation

Data about fluorescence cross-sections due to excitation/ionization through electrons can be obtained from [5]. In the case of radiation emitted by N₂ around 337 nm the cross-section drops for electron energies above a few tens of eV according to:

$$\sigma_{337}^e = A_2 \cdot E^{-2} \quad (4)$$

with $A_2 = 1.48 \cdot 10^{-15} \text{ cm}^2 \cdot \text{eV}^2$. Thus for 10 keV electrons one would expect $\sigma_{337}^e \approx 1.48 \cdot 10^{-23} \text{ cm}^2$.

The cross-section for light emission due to N₂⁺ behaves at electron energies above 100 eV according to the Bethe–Oppenheimer approximation [6]:

$$\sigma_{391}^e = A_3 \cdot E^{-1} \cdot \ln(B_3 \cdot E) \quad (5)$$

with $A_3 = 1.66 \cdot 10^{-15} \text{ cm}^2 \cdot \text{eV}$ and $B_3 = 2.4 \cdot 10^{-2} \text{ eV}^{-1}$. Hence at 10 keV one obtains $\sigma_{391}^e \approx 9.1 \cdot 10^{-19} \text{ cm}^2$.

Integration Times

We will take the following parameters into consideration for the estimation of the integration times needed to obtain a proper image of the interaction region between the charged particle beams and the gas jet curtain: a gas number density $n = 2.5 \cdot 10^{10} \text{ cm}^{-3}$, a curtain thickness $d = 0.5 \text{ mm}$, $T = 0.65$ transmittance of the optical system including windows, a transmittance $T_f = 0.3$ of an optical filter within its transmission band, an acceptance solid angle $\Omega = 4\pi \cdot 10^{-5} \text{ sr}$, an efficiency η_{pc} of the MCP's photocathode of 20% and a detection efficiency η_{MCP} of the MCP of 50%. Since the integration time scales inverse proportionally with the (average) charged particle current, we will consider $I = 1 \text{ A}$. Thus the average number of photons detected within a time Δt is given by:

$$N_\gamma = \sigma \cdot \frac{I \cdot \Delta t}{e} \cdot n \cdot d \cdot \frac{\Omega}{4\pi} \cdot T \cdot T_f \cdot \eta_{pc} \cdot \eta_{MCP} \quad (6)$$

With the assumed numerical values $N_\gamma \approx 1.5 \cdot 10^{21} \cdot \sigma \cdot \Delta t$, with $[\sigma] = \text{cm}^2$ and $[\Delta t] = \text{s}$. In case of proton excitation this results in an average time of 20 ms/photon, while for excitation through electrons this is 0.7 ms/photon. The average integration time corresponding to the emission due to the neutral molecule turns out to be prohibitively large: 45.5 s/photon.

BIF based beam diagnostics performed at GSI showed that a few hundred of photons are usually enough for obtaining well defined profiles. Thus one would expect that an integration time of up to about 10 s is needed to obtain an adequate signal from the proton beam, while a few hundred of milliseconds would be sufficient for detecting the electron beam.

Secondary Electrons

The analysis above considered just the primary beams. However, due to the strong longitudinal magnetic field low energy secondary electrons produced through ionization of the gas curtain and background gas molecules will be forced to gyrate around the magnetic field lines while also suffering a $\mathbf{E} \times \mathbf{B}$ drift on circular average trajectories around the beam axis. For the sake of simplicity we will neglect here the $\mathbf{E} \times \mathbf{B}$ drift.

Most of the secondary electrons produced by ionization due to relativistic protons have their momenta oriented almost perpendicular to the one of the projectile [7]. The energies of these electrons may exceed 100 eV, nonetheless most of them have energies below this value. As an example we consider a 30 eV electron in a homogeneous magnetic field and assume that just 0.1% of its energy is due to the longitudinal movement. This results in a time needed to pass through the gas curtain of about 5 ns during which the electron would actually travel over approximately 16 mm, due to its gyration movement. For the cross-section we consider the average between σ_{337}^e and σ_{391}^e at 30 eV, since according to [5] they are of the same order of magnitude. Hence its value is $\bar{\sigma}^e \approx 3.8 \cdot 10^{-18} \text{ cm}^2$.

Under these conditions secondary electrons have the potential to generate much more photons than the primary protons. Yet, to estimate the number of photons that would originate from these electrons, one has to evaluate the amount of secondary electrons passing the gas curtain per unit time. To this end the background gas has to be taken into consideration. The mean free path of secondary electrons at a pressure of about 10^{-8} mbar is of the order of 10 km along the magnetic field lines if one considers for instance the ionization cross-section of about 10^{-16} cm^2 . Therefore they can reach the curtain, even if generated far away from it.

In a steady state situation, by neglecting any other contributions besides ionizations produced within the homogeneous field region, the electron flux through the ends of this region would amount the number of electrons generated inside it per unit time. For estimation purposes we consider just 1 m length and an ionization cross-section of about 10^{-18} cm^2 due to the protons [4]. Taking into account that approximately 50% of the electrons have their momenta towards the gas curtain the secondary electron current has a value of about $1.25 \cdot 10^{-8} \text{ A}$, far too low to allow for a significant contribution from these electrons, even with the increased cross-section and path travelled within the gas curtain.

The situation is similar in the case of fluorescence at 391 nm and secondary electrons generated by the main electron beam. However, the cross-section for the generation of radiation at 337 nm by electrons at few tens of eV is five orders of magnitude higher than the one of the primary electrons. In addition, by using the Bethe–Oppenheimer approximation for extrapolating the data in [5] the ionization cross-section for 10 keV electrons estimates to 10^{-17} cm^2 , one order of magnitude higher than for 7 TeV protons. Finally, from the double differential cross section data published in [8] for 2 keV electrons, one may expect that secondary electrons are predominantly generated in forward direction. Thus, with proper placement of the gas curtain and an accumulation length larger than 1 m, the amount of radiation generated by secondary electrons may become of the same order of magnitude as the one due to the primary ones. If one succeeds to also increase Ω by a factor of 10 the specific integration time at 337 nm would drop to about 2.3 s/photon, for a primary current of 1 A. Besides, the integration time can be further reduced, if a higher

background gas pressure can be allowed and a reduction of the primary electron beam energy may be afforded. Hence, one may conclude that making use of fluorescence arising from neutral nitrogen has to rely on secondary, low energy electrons.

THE OPTICAL SYSTEM

The optical system has to fulfil certain conditions, resulting from the experimental demands. It should have a large acceptance solid angle and high transmittance. When positioned at an angle with respect to the gas curtain, it should allow for a depth of field (DOF) of at least 5 mm, which would also ensure proper imaging if the beams are slightly displaced from the ideal position. Because of the small transversal sizes of the proton and electron beams and the relatively low resolution of the MCP detector of about 20 lp/mm, it should provide a magnification close to ± 1 . Finally, the field of view should have a diameter not below 15 mm.

Within the paraxial approximation, and considering a relatively small DOF the maximum diameter Φ_{\max} of a spot at the detector corresponding to a point source in the image plane is related to the magnification β , the acceptance solid angle Ω and the DOF as follows:

$$\Phi_{\max} = \frac{\text{DOF}}{\sqrt{\pi}} \cdot \sqrt{\Omega} \cdot |\beta| \quad (7)$$

Thus one cannot increase acceptance and/or magnification without reducing the DOF, if the blur of the image is to be kept below a certain level.

Presently three types of systems which can be realized from off the shelf parts are under consideration:

- a single corrected triplet optimized for $\beta = -1$ and having a focal length of 200 mm
- three corrected triplets each optimized for $\beta = -1$ and having a focal length of 120 mm
- three corrected triplets, the first with a focal length of 100 mm and the other two both with a focal length of 50 mm

The first two systems have the advantage of a large acceptance solid angle of about $4\pi \cdot 10^{-4}$ sr at $\beta = \pm 1$ but are inflexible. The third system has a higher flexibility, but a lower acceptance of about $8\pi \cdot 10^{-5}$ sr and a magnification of 0.85. More detailed computations are ongoing to assess the residual geometric and chromatic aberrations and allow for a final decision.

PARTICLE DYNAMICS

As shown earlier in this article, most of the radiation is emitted by N_2^+ . The corresponding excited states have a life time of about 60 ns [4]. During this time the ions move under the influence of the strong longitudinal magnetic field and the electric fields of the proton and electron beams. To study the movement of the ions under the given conditions a software got implemented based on the numerical tools provided by the numpy and scipy libraries [9].

The DC annular electron beam has a transversal profile which is flat between the inner radius and the outer one. The beam is considered to have only transversal components of the electric field. Its own magnetic field is also neglected.

ISBN 978-3-95450-177-9

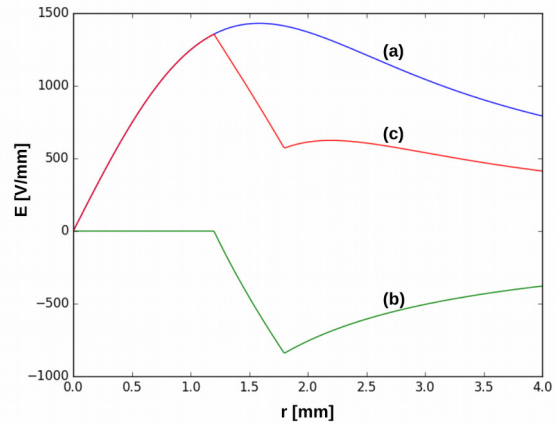


Figure 2: The transverse electric fields: (a) proton bunch at highest charge density, a total of $2.2 \cdot 10^{11}$ protons and 2.4 mm FWHM, (b) electron beam with a current of 5 A and 10 keV electrons, $\Phi_{\text{in}} = 2.4$, $\Phi_{\text{out}} = 3.6$ mm (c) superposition of the two fields.

The LHC beam is modelled as a train of bunches with a frequency of 40 MHz. Each bunch has a parabolic longitudinal profile with a total duration of 1 ns and a Gaussian transversal profile. Because of the very high proton energy, just the transversal component of the electric field is taken into consideration, while the beam's magnetic field is neglected, since it is much smaller than the external 4 T solenoid field. Fig. 2 shows the transverse electric fields and their superposition.

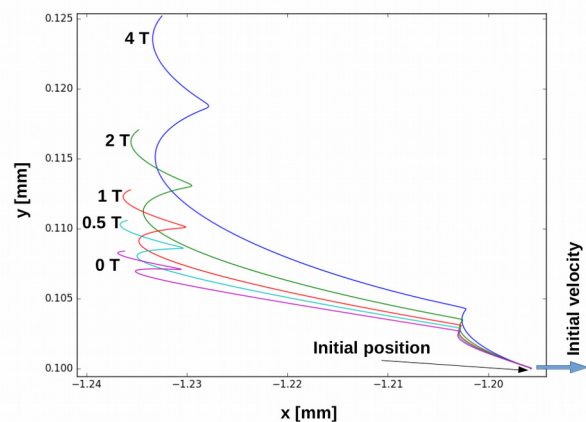


Figure 3: N_2^+ trajectories for different solenoid field strengths. The axis of the two beams is out of this image, at (0, 0). The tracking lasts for 60 ns and one can observe the effect due to proton bunches passing by. Beam parameters as for Fig. 2.

The influence of the solenoid magnetic field on the movement of an N_2^+ ion produced at the inner radius of the annular electron beam is illustrated in Fig. 3. The tracking time is 60 ns. The ion has an initial velocity of 1 km/s, close to typical values for gas jet curtains [10]. This velocity changes very quickly due to the high field intensities. The magnetic field induces a drift which makes the ion move further from the initial position than

in its absence. The maximum displacement is of a few tens of micrometers.

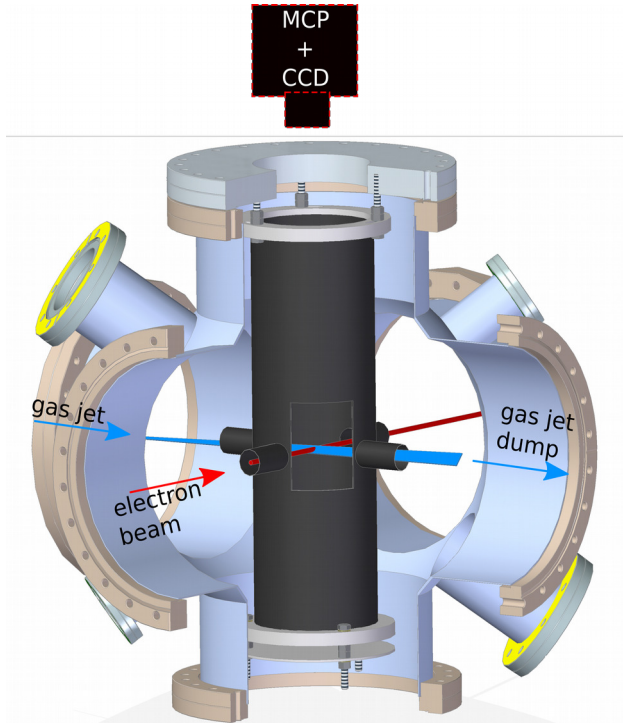


Figure 4: Schematic of the experimental setup at the Cockcroft Institute. The blackened insertion chamber has five lateral openings, two pairs for the gas jet curtain and the electron beam respectively and one for introducing a scintillator.

EXPERIMENTAL TEST SETUP

An experimental test setup has been realized at the Cockcroft Institute for first experiments to verify the predictions with respect to the photon yield and also investigate the possibility of using neon instead of nitrogen. The setup consists of a gas jet system [2, 10] capable to produce a curtain with a width of several millimetres, a sub-millimetre thickness and a particle density of about 10^{10} cm^{-3} , an electron gun delivering up to $10 \mu\text{A}$ and a maximum energy of 5 keV, an ICCD camera and a filter wheel with interference filters with a bandwidth of 10 nm and central wavelengths at 337, 391, 431 and 471 nm. Moreover a dedicated, blackened insertion chamber has been designed, constructed and installed in the main experimental chamber to reduce stray light. A schematic of the setup is shown in Fig. 4. Commissioning of the setup showed that the main issue are the very long integration times needed due to the low electron beam current. This makes the proper relative alignment of the electron beam with respect to the gas jet very tedious. Measurements are planned for the fall 2016 after completion of the setup's adjustment.

CONCLUSIONS

Production rates and corresponding integration times for photons emitted by N_2 and N_2^+ at 337 and 391 nm respectively have been assessed based on available cross-

section data and extrapolation formulas. It has been shown that most of the fluorescence signal is due to N_2^+ and that the primary electron beam at 10 keV leads to a much weaker emission from N_2 . Hence the contribution of excitations by secondary, low energy electrons has been investigated, with the result that they may considerably increase the fluorescence signal at 337 nm.

Numerical tracking of N_2^+ ions in the relevant electric and magnetic fields showed that during the life time of the excited level and under the assumed initial conditions they do not move by more than about $40 \mu\text{m}$ from the position at which they got ionized. This distance is much smaller than the beam sizes involved and should only weakly affect the profile measurement.

An experimental test setup has been commissioned at the Cockcroft Institute and is available for first experiments to check the theoretical predictions with respect to photon production rates.

ACKNOWLEDGEMENT

The authors would like to acknowledge fruitful discussions with D. Vilsmeier and M. Sapinski.

REFERENCES

- [1] V. Shiltsev, V. Danilov, D. Finley, and A. Seryus, "Considerations on compensation of beam-beam effects in the Tevatron with electron beams", *Phys. Rev. ST Accel. Beams*, vol. 2, p. 071001, Jul. 1999.
- [2] V. Tzoganis and C. P. Welsch, "A non-invasive beam profile monitor for charged particle beams", *Appl. Phys. Lett.*, vol. 104, p. 204104, May 2014.
- [3] F. Becker, "Non-destructive Profile Measurement of intense Ion Beams", Ph.D. thesis, Phys. Dept., Technische Universität Darmstadt, Germany, 2009.
- [4] M. A. Plum, E. Bravin, J. Bossert, and R. Maccaferri, " N_2 and Xe gas scintillation cross-section, spectrum, and lifetime measurements from 50 MeV to 25 GeV at the CERN PS and Booster", *Nucl. Instr. Meth. A*, vol. 492, pp. 74-90, 2002.
- [5] Y. Itikawa, "Cross Sections for Electron Collisions with Nitrogen Molecules", *J. Phys. Chem. Ref. Data*, vol. 35, pp. 31-53, 2006.
- [6] W. L. Borst and E. C. Zipf, "Cross Section for Electron-Impact Excitation of the (0,0) First Negative Band of N_2^+ from Threshold to 3 keV", *Phys. Rev. A*, vol. 1, pp. 834-840, Mar. 1970.
- [7] A. B. Voitkiv, N. Gruen, and W. Scheid, "Hydrogen and helium ionization by relativistic projectiles in collisions with small momentum transfer", *J. Phys. B: At. Mol. Opt. Phys.*, vol. 32, pp. 3923-3937, 1999.
- [8] R. R. Goroganthu, W. G. Wilson, and R. A. Bonham, "Secondary-electron-production cross sections for electron-impact ionization of molecular nitrogen", *Phys. Rev. A*, vol. 35, pp. 540-558, Jan. 1987.
- [9] S. van der Walt, S. C. Colbert, and G. Varoquaux, "The NumPy Array: A Structure for Efficient Numerical Computation", *Comp. in Sci. & Eng.*, vol. 13, pp. 22-30, 2011.
- [10] H. Zhang, V. Tzoganis, A. Jeff, A. Alexandrova, and C. P. Welsch, "Characterizing Supersonic Gas Jet-Based Beam Profile Monitors", in *Proc. IPAC'16*, Busan, Korea, May 2016, paper MOPMR046, pp. 357-360.